

## Optical modulator with ZnO bulk single crystals

Sabah Al-ithawi

*University of Technology –Baghdad -Iraq*

Received 5 Apr 2017; Revised 19 May 2017; Accepted 22 May 2017

### Abstract

An optical modulator was fabricated with semiconductor ZnO by associating a nematic liquid crystal layer with indium–tin oxide. This device revealed the height variation in the phase and refractive index of irradiation ultraviolet laser light ( $\lambda = 375$  nm) as well as in the voltage applied. This new optical modulator operated efficiently in the infrared range up to 4  $\mu\text{m}$ .

**Keywords:** Electro-optical Modulator, Indium Tin Oxide (ITO), ZnO n-type semiconductor, liquid crystals (LCs), metal-insulator-semiconductor (MIS) structure.

### 1. Introduction

The semiconductor ZnO is a promising material and has been widely used recently, as evidenced by the increase in the number of its applications. The interest in ZnO is due to its direct wide band gap (e.g.,  $\sim 3.3$  eV at 300 K) and large exciton binding energy ( $\sim 60$  eV). However, ZnO possesses the same crystal structure as GaN, although the former presents advantages over the latter; these advantages include the availability of high-quality ZnO bulk single crystals [1–4]. Furthermore, ZnO possesses a much simpler crystal-growth trend than GaN, so ZnO-based devices are less expensive than GaN devices. The chemical stability of ZnO is very high, such that ZnO is regarded as a green material. However, ZnO exhibits transparency and contains many crystalline structures, such as rock salt, zinc blend, and wurtzite (Fig. 1). The wurtzite structure presents interesting properties because of its thermodynamic stability under ambient temperature.

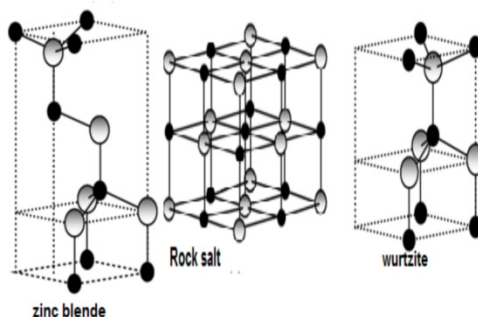


Fig.1: Crystallizes structures of ZnO [4]

\*For Correspondence. E-mail: sa\_laser@yahoo.com

Bulk single-crystal ZnO can be grown through various techniques, such as vapor-phase transport, hydrothermal growth, and pressurized melt growth. The difference between bulk and thin-film crystals lies in size. Bulk crystals have sizes of up to 2 inches [5–10]. We measured the absorption coefficient of bulk single-crystal ZnO (Fig. 2) and found that light could be absorbed in the ultraviolet region. We used liquid crystals (LCs) with interesting properties, such as sensitivity to the external field and high birefringence [11–13]. In addition, indium–tin oxide (ITO) was utilized as the transparent conductor. The proposed optical modulator with a metal–isolator–semiconductor architecture demonstrated good performance.

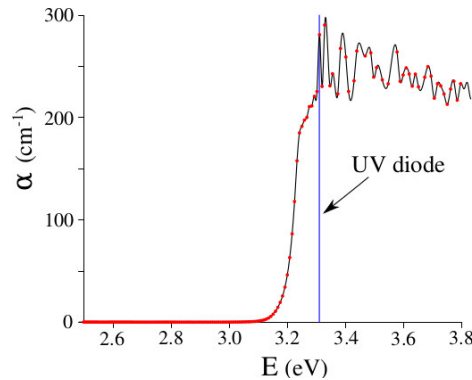


Fig. 2: The absorption spectrum of ZnO

## 2. Experimental

### Electrical conductivity and photoconductivity of ZnO

The large-band-gap material of ZnO allows for the use of ZnO in many applications such as electronics and optoelectronics (Figure 3) and results in many advantages, such as high breakdown voltage, low noise generation, and suitable for high temperatures and high-power operations. The doped n-type ZnO, with  $ND \sim 10^{16} \text{ cm}^{-3}$  at ambient temperature was utilized as the conductor.

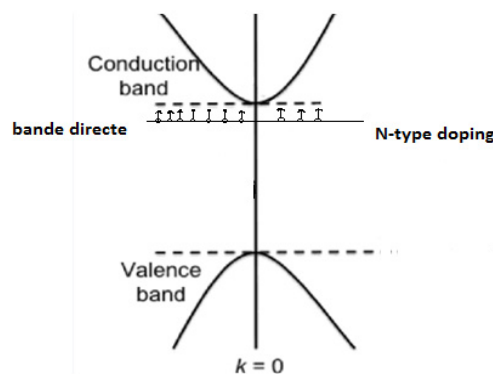


Fig. 3: The energy diagram for ZnO -n type

In the doped semiconductor, the n-type electron mobility strongly varied with the temperature and was very sensitive to an electric field [14]. The electron absorbed electric or thermal energy and transmitted it from the valence band to the conduction band. When the photon energy was greater than the energy gap of ZnO, a pair of free-electron holes was created. The density of the photo carriers increased ( $P+\Delta P$ ) due to the density of the holes. Hence, conductivity increased with irradiation.

$$\sigma_0 + \Delta \sigma(I) = \sigma \tag{1}$$

The initial thermal-equilibrium conductivity was obtained as  $\sigma_0 = ND \times e\mu_n$ , where  $ND$  represents the density of the electron in  $\text{cm}^3$  and  $\mu_n$  represents the mobility of the electron. A voltage drop would create an electric field and generate current.

$$J = \sigma E \tag{2}$$

We characterized the electrical conductivity after fabricating a contact metal–semiconductor of Ag–ZnO as shown in Fig. 4.

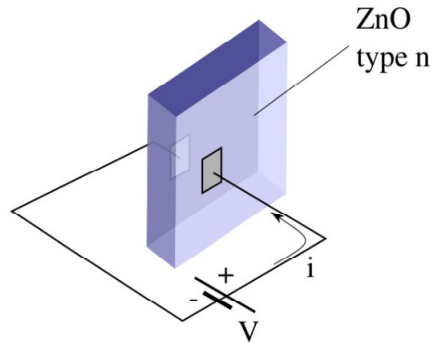


Fig. 4: Voltage drop across ZnO by Ag metal contact

The results in Fig. 4 indicate that Ohm’s law was not well followed. Therefore, the electrical contact was not perfectly ohmic, as shown in Figs. 5 and 6.

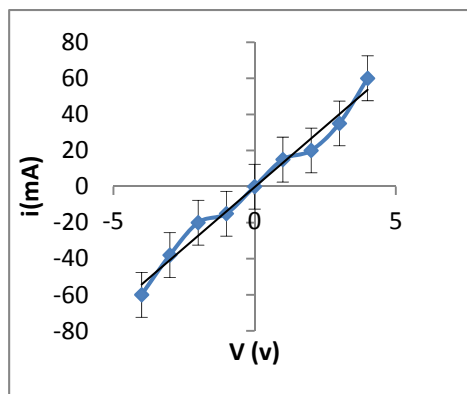


Fig. 5: Measured the current as a function of the voltage applied, it’s shown not aligned with the sold line, so Ohm's law is not well followed.

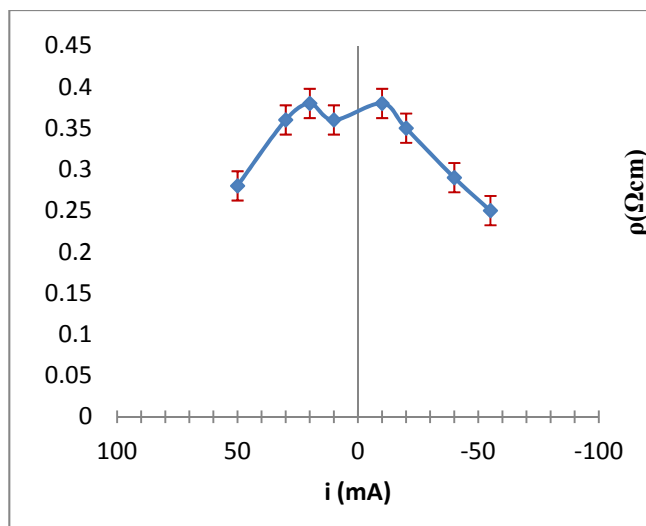


Fig. 6: Measured resistance as a function of the current, we measured ( $\rho$ ) from  $\rho = (v*s)/(I*d)$ , where (s, d) present length and width of the ZnO sample.

After measuring the electrical conductivity, we measured the photoconductivity of ZnO under irradiation by ultraviolet laser light at a wavelength of 375 nm as shown in Fig. 7. Conductivity and current increased, and we can use the form:

$$i = i_0 + \Delta i(I_{uv}) \tag{3}$$

The results obtained as plotted in Fig. 8.

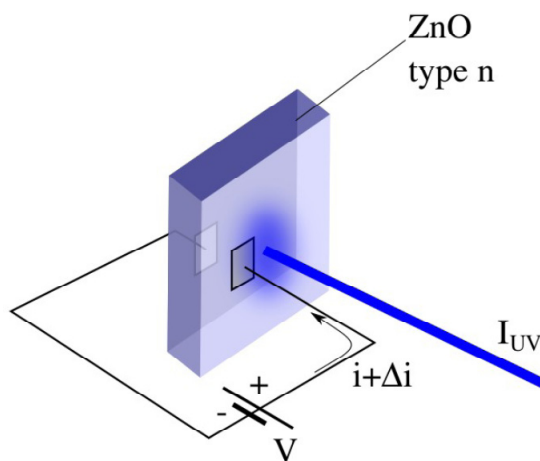


Fig. 7: ZnO under irradiation at  $\lambda = 375 \text{ nm}$

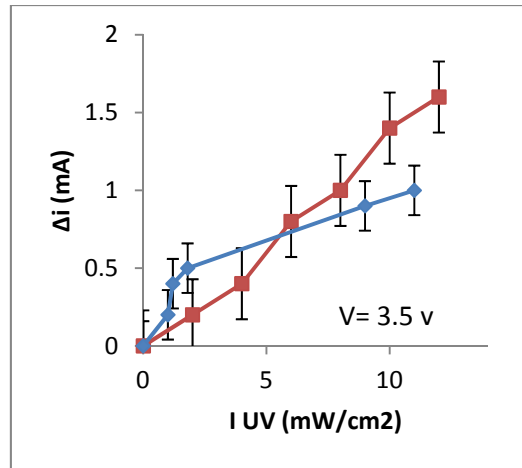


Fig. 8: The variation of current under irradiation

### 3. Fabrication and characterization of an optical modulator

An optical modulator is an instrument for manipulating a property of light. We fabricated an optical modulator composed of two slides. The first slide is the bulk crystal of ZnO, and the second slide is the composition of ITO with transparent glass on the other side. The distance between the slides is  $9\ \mu\text{m}$ . After scarification of the surface of ITO, it was filled with LCs to fix the molecules on the surface. The nematic type of LCs (E48, Merck) was used. The birefringence of E48 was  $n = n_e - n_o = 0.16$ , where ordinary indices of refraction  $n_o = 1.54$  and extraordinary indices of refraction  $n_e = 1.7$  (equal dielectric anisotropy  $\Delta\varepsilon = 15.1$  at 1.0 kHz). We connected the two slides with silver metal (Ag), as shown in Fig. 9. This structure is called a metal–isolator–semiconductor (MIS).

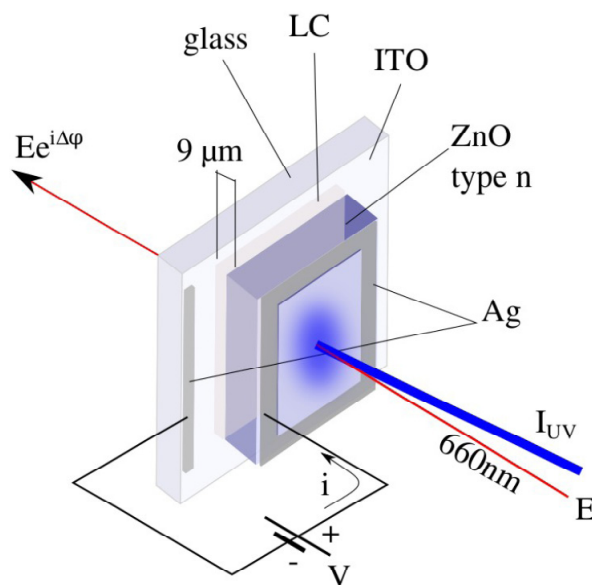


Fig. 9: Optical modulator by structure MIS

The refractive index of liquid crystal is changed with the voltage applied.

#### 4. Optical phase modulator

A 660 nm reading laser was allowed to pass through the cell and linearly polarized along the LC direction (Fig. 10). No changes were observed.

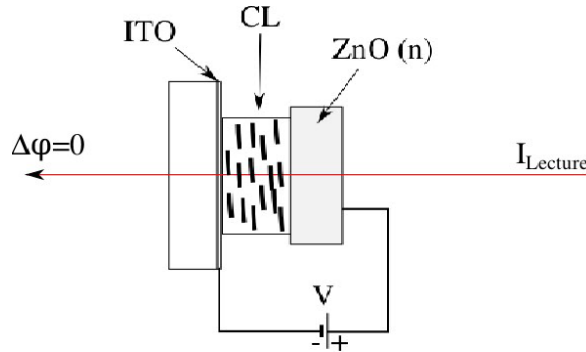


Fig. 10: Optical modulator irradiate by 632 nm

Under ultraviolet illumination, loads were created at the interface of LC–ZnO (Fig. 11), and the voltage applied:

$$V(t)=V_0\sin(2\pi ft) \tag{4}$$

At the electrodes, ITO–ZnO permitted the reorientation of the molecules of the LC. The reading laser had a phase shift, which relied on the intensity of the ultraviolet laser.

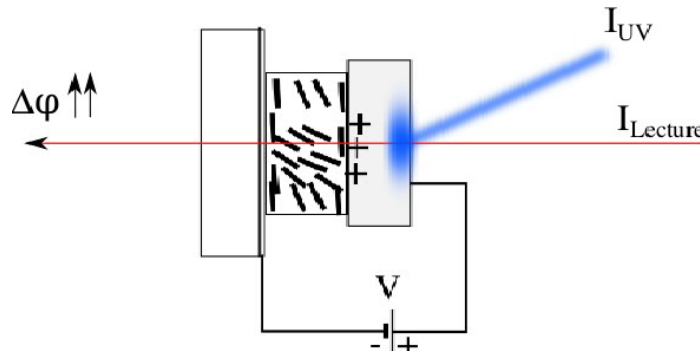


Fig. 11: Optical modulator irradiate by 375 nm

#### 5. Phase shift measurements

The beam of light that transited over the MIS gained a phase shift  $\Delta\phi$  that relied on the voltage applied  $v(t)$  and the intensity of the fallen beam itself. The produced phase shift can be expressed in the following form

$$\Delta\phi=2\pi/\lambda*d*\Delta n \tag{5}$$

where  $\Delta n = n_e(\theta) - n_o$ . With  $\theta$ , a local angle was created from the LC direction in consideration of the perpendicular axis. For  $\theta=0$ , we have  $n_e(0) = n_e$ , and for  $\theta = \pi/2$ , we have  $n_e(\pi/2) = n_o$ . The entire term flow equations are;

$$n_e(\theta) = n_e n_o / \text{SQRT} (n_e^2 \sin^2(\theta) + n_o^2 \cos^2(\theta)) \tag{6}$$

Under threshold  $\theta (0)$ , the output phase is  $2\pi d n_e / \lambda$

When a high-intensity laser or high voltage is used, the saturation of the local angle ( $\theta$ ) reaches  $\pi/2$ , and the output phase is  $2\pi d n_o / \lambda$  [10–14]. The produced phase shift reaches the maximum value when a light with strong intensity is used, and this in turn saturates the MIS response to  $2\pi d (n_o - n_e) / \lambda = 14$  rad. To measure the phase shift, the MIS must be placed between two crossed polarizers. The direction should be oriented at  $45^\circ$  of the perpendicular axis. In this condition, the relation between output intensity and phase shift is directly proportional, namely,  $I_{\text{out}} \propto I / 2 [1 - \cos(\Delta\phi)]$ , for measuring phase shift. This is achieved by calculating the output intensity, as shown in Fig. 12.

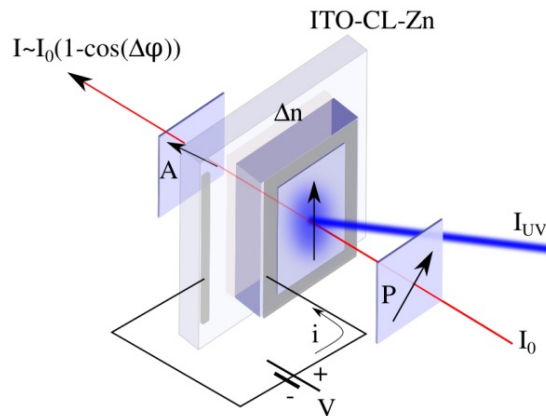


Fig. 12: Optical modulator (MIS) with two crossed polarizers for measured  $\Delta\phi$

$$I = I_0 (1 - \cos(\Delta\phi))$$

From the current measurement, we can calculate the phase shift. So the result as in Fig. 13 and 14.

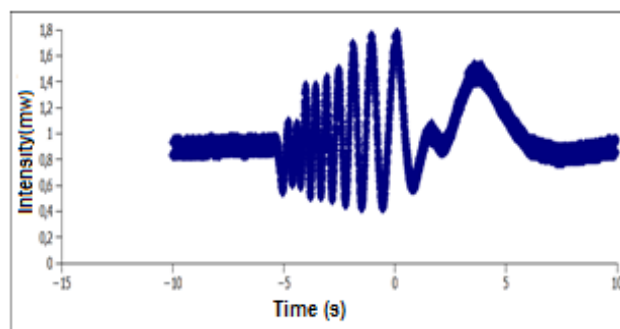


Fig. 13: The phase shift measured directly by oscilloscope, voltage drop 15 vdc

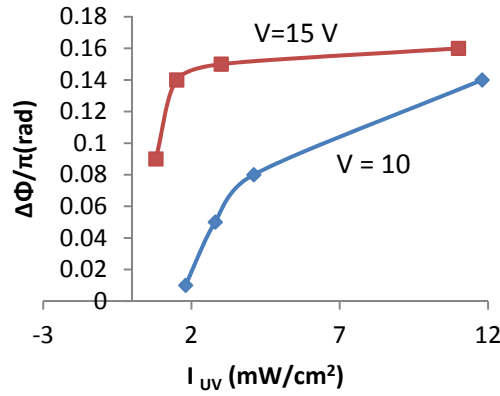


Fig. 14: The Measured phase shift as a function of different voltage drop and intensity

### 6. Measurement of the refractive index

We measured the refractive index ( $\Delta n$ ) by using the same arrangement as that in Fig. 12 and calculated the following:

$$\Delta n = \lambda/2\pi d * \Delta\phi$$

The result obtained as shown in Fig. 15.

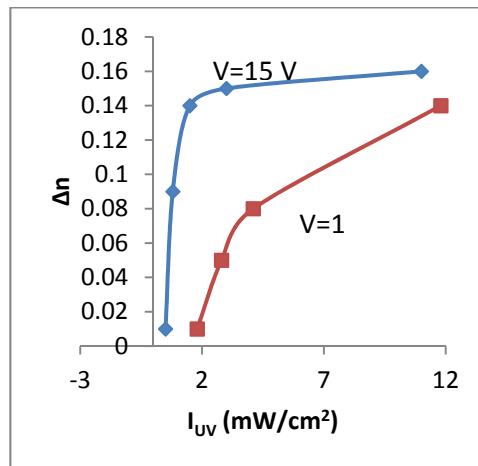


Fig. 15: The relationship between a light intensity and the measured the change of refractive index  $\Delta n$  for different voltage applied V

### 7. Measurement of the response time

Response time depends on electron concentration. We estimated  $\tau_{ph}$  from the mode operation (off/on/off mode). The maximum voltage applied was 20 V, as shown in Fig. 16.



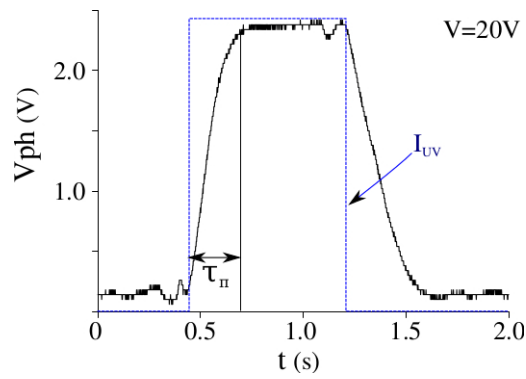


Fig. 16: Estimated response time by operation mode off/on/off under irradiation  $I_{uv}$  and voltage drop 20 V

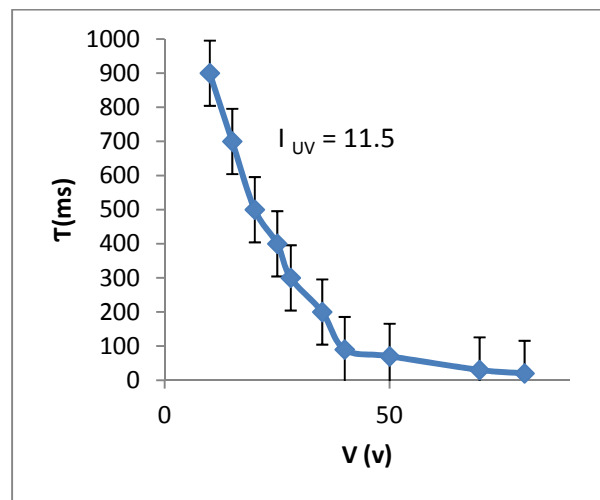


Fig. 17: Measured response time as a function of different applied voltage  $V$

## 8. Conclusion

We characterized the electrical conductivity and photoconductivity of n-doped ZnO crystal. We fabricated a new optical phase modulator consisting of a nematic LC layer connected to ZnO:ITO and used Ag for ohmic contact interdigitated electrodes. Phase shift was controlled by an ultraviolet laser and can be evaluated by the thickness of the layer and the birefringence of the nematic. We discovered that the variation index is very high (0.16), with a response time in the order of tens of milliseconds.

## Acknowledgements

This work has been supported by the University of Nice Sophia Antipolis in the laboratory (INLN) Nice, France and supported by projects (UVSLM)) GISAzur Opto, The authors are also acknowledged to U. Bortolozzo, S. Residori .

## References

- [1] U. Ozgur, Ya. L. Alivov, Chunli. L, H. Morkoc. (2005). *Applied Physics.Rev.* **98**, 041301
- [2] H. Ohta, M. Hirano, K. Nakahara, H. Maruta, T. Tanabe, M. Kamiya, T. Kamiya, H. Hosono. (2003). *Appl. Phys. Lett.*, 83 (5), 4 August
- [3] C. F. Klingshirn, A. Waag, A. Hoffmann and J. Geurts. (2010). Springer
- [4] V. Avrutin, G. Cantwell, J. Z. Zhang, J. J. Song, D. J. Silversmith and H. Morkoc. (2010). *Proceedings of the Ieee*, **98**, 1339-1350
- [5] A. Janotti , C. G Van de Walle. (2009). *Rep. Prog. Phys.* **72**, 126501, pp.29
- [6] H. Morkoç , Ü. Özgür . (2009). ISBN: 978-3-527-40813-9, Wiley
- [7] K. Maeda, M. Sato, I. Niikura and T. Fukuda. (2005). *Semiconductor Science and Technology*, 20, S49-S54
- [8] X. Zhang, F. Herklotz, E. Hieckmann, J. Weber and P. Schmidt. (2011). *Journal of Vacuum Science & Technology A* **29**, 03A107
- [9] P. Skupinski, K. Graszka, A. Mycielski, W. Paszkowicz, E. Lusakowska, E. Tymicki, R. Jakiela and B. Witkowski. (2010). *Physica Status Solidi B-Basic Solid State Physics*, **247**, 1457-1459
- [10] L. N. Dem'yanets and V. I. Lyutin. (2008). *Journal of Crystal Growth*, **310**, 993-999.
- [11] H. mathieu, H. Fanet. (2009). 6th editor
- [12] E. Rosencher, B. Vinter. (2002). DUNOD , 2<sup>nd</sup> editor
- [13] I. C. Khoo. (2007). Wiley-Interscience, 2nd ed
- [14] U. Bortolozzo, S. Residori, Jean-Pierre Huignard. (2013). **52**, (22) / *APPLIED OPTICS E73*, 1 August
- [15] D. K. Yang, S. T. Wu. (2006). Wiley
- [16] K. liu, M. Sakurai, M. Anon. (2010). **10** (9), 8604-8634, *Sensors*
- [17] K. W. Liu, J. G. Ma, J. Y. Zhang, Y. M. Lu, D.Y. Jiang, B.H. Li a, D. X. Zhao, Z. Z. Zhang, B. Yao, D. Z. Shen. (2007). *Solid-State Electronics* **51**, 757-761
- [18] B. Boruah. (2009). *Am. J. Phys.* **77**, 331-336
- [19] J. Pavlin, N. Vaupotič, and M. Čepič. (2003). *Eur. J. Phys.* **34**, 745-761
- [20] D. Huang, H. Timmers, A. Roberts, N. Shivaram, and A. S. Sandhu. (2012). *Am. J. Phys.* **80**, 211-215
- [21] V. Arrizón. (2003). *Opt. Lett.* **28**, 1359-1361
- [22] E. G. Van Putten, I. M. Vellekoop and A. P. Mosk. (2008). *Appl. Opt.* **47**, 2076-2081
- [23] M.J.Weber. (2003). *Handbook of optical materials*, CRC Press
- [24] Atul Gupta, H. S. Bhatti, D. Kumar, N. K. Vermaa , R. P. Tandonb. (2006). *Digest Journal of Nanomaterials and Biostructures*, **1**, 1, March
- [25] S. Chu, M. Olmedo, Z. Yang, J. Y. Kong and J. L. Liu, (2008). *Applied Physics Letters*, **93**, 181106
- [26] L. N. Dem'yanets and V. I. Lyutin. (2008). *Applied Physics Letters*, **93**, 181106
- [27] K. Jacobs, D. Schulz, D. Klimm and S. Ganschow. (2010). *Solid State Sciences*, 12, 307-310